Natural Resources Canada
Ressources naturelles Canada

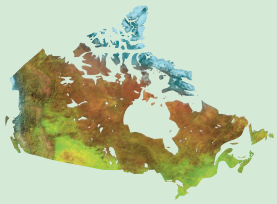

# Totnes Road metavolcanic rocks: a fragmental, Ti-enriched komatiitic volcanic suite on Cumberland Peninsula, Baffin Island, Nunavut

*R.D. Keim, M. Sanborn-Barrie, K. Ansdell, and M. Young*

Geological Survey of Canada

Current Research 2011-13

2011

Canada

Geological Survey of Canada
Current Research 2011-13

# Totnes Road metavolcanic rocks: a fragmental, Ti-enriched komatiitic volcanic suite on Cumberland Peninsula, Baffin Island, Nunavut

*R.D. Keim, M. Sanborn-Barrie, K. Ansdell, and M. Young*

2011

ISSN 1701-4387
Catalogue No. M44-2011/13E-PDF
ISBN 978-1-100-18727-3
doi: 10.4095/289072

A copy of this publication is also available for reference in depository libraries across Canada through access to the Depository Services Program's Web site at http://dsp-psd.pwgsc.gc.ca

A free digital download of this publication is available from GeoPub:
http://geopub.nrcan.gc.ca/index_e.php
Toll-free (Canada and U.S.A.): 1-888-252-4301

**Recommended citation**
Keim, R.D., Sanborn-Barrie, M., Ansdell, K., and Young, M., 2011. Totnes Road metavolcanic rocks: a fragmental, Ti-enriched komatiitic volcanic suite on Cumberland Peninsula, Baffin Island, Nunavut; Geological Survey of Canada, Current Research 2011-13, 18 p. doi:10.4095/289072

***Critical review***
*J. Percival*

***Authors***
***R.D. Keim (rdk503@mail.usask.ca)***
***K. Ansdell (kevin.ansdell@usask.ca)***
*Department of Geological Sciences*
*University of Saskatchewan*
*114 Science Place*
*Saskatoon, Saskatchewan, S7N 5E2*

***M. Sanborn-Barrie***
***(Mary.Sanborn-Barrie@NRCan-RNCan.gc.ca)***
*Geological Survey of Canada*
*601 Booth Street*
*Ottawa, Ontario, K1A OE8*

***M. Young (MDYoung@Dal.Ca)***
*Dalhousie University*
*Edzell Castle Circle*
*Halifax, Nova Scotia, B3H 4J1*

Correction date:

# Totnes Road metavolcanic rocks: a fragmental, Ti-enriched komatiitic volcanic suite on Cumberland Peninsula, Baffin Island, Nunavut

R.D. Keim, M. Sanborn-Barrie, K. Ansdell, and M. Young

Keim, R.D., Sanborn-Barrie, M., Ansdell, K., and Young, M., 2011. Totnes Road metavolcanic rocks: a fragmental, Ti-enriched komatiitic volcanic suite on Cumberland Peninsula, Baffin Island, Nunavut; Geological Survey of Canada, Current Research 2011-13, 18 p. doi:10.4095/289072

**Abstract:** A distinctive sequence of fragmental komatiite and komatiitic basalt exposed on Cumberland Peninsula, eastern Baffin Island, is thought to be part of the Paleoproterozoic Hoare Bay Group. Its fragmental nature suggests the actions of steam and magmatic explosivity of ultramafic magma under relatively shallow water. Its Al-undepleted geochemical character suggests a parental magma derived from shallow-mantle melting at pressures of 4 to 6 GPa, while its Ti, high field-strength element (HFSE), and LREE-enrichment suggest retention of the first melt increment or modification of the parental magma during its ascent to surface. Collectively, the textural and compositional characteristics are consistent with Karasjok-type komatiites — a Ti-enriched komatiitic composition first described from the Karasjok Greenstone Belt in Finland. The Totnes Road komatiites are associated with clastic and chemical metasedimentary rocks, an association documented at other localities on Cumberland Peninsula.

**Résumé :** Une séquence caractéristique de komatiite et de basalte komatiitique fragmentaires affleurant dans la péninsule Cumberland, dans l'est de l'île de Baffin, appartiendrait, selon notre interprétation, au Groupe de Hoare Bay du Paléoprotérozoïque. Sa nature fragmentaire suggère une explosivité magmatique du magma ultramafique et une explosivité de vapeur dans des eaux relativement peu profondes. Sa composition géochimique non appauvrie en Al laisse supposer un magma parental dérivé d'une fusion du manteau peu profond dans des conditions de pression de 4 à 6 GPa, tandis que son enrichissement en Ti, en éléments à fort effet de champ et en terres rares légères suggère la rétention du premier incrément de fusion ou la modification du magma parental pendant sa remontée vers la surface. Dans l'ensemble, les caractéristiques texturales et compositionnelles sont cohérentes avec les komatiites de type Karasjok, une composition komatiitique enrichie en Ti décrite pour la première fois d'après la ceinture de roches vertes de Karasjok, en Finlande. Les komatiites de Totnes Road sont associées à des roches métasédimentaires clastiques et chimiques, une association documentée à d'autres endroits dans la péninsule Cumberland.

## INTRODUCTION

The Cumberland Peninsula Integrated Geoscience project was launched in 2008 under the Government of Canada's Geo-mapping for Energy and Minerals (GEM) initiative in order to address the significant geoscience knowledge gap that existed due to limited and outdated mapping for this extensive region (Jackson and Taylor, 1972) . This has been accomplished through acquisition of high-resolution aeromagnetic data (Coyle, 2009a, b, c) and systematic surficial (Dyke, in press a, b, c; Gammon et al., 2011) and bedrock (Sanborn-Barrie et al., 2010, 2011) mapping across the peninsula during the summers of 2009 and 2010. This research contribution highlights a distinctive sequence of ultramafic metavolcanic rocks exposed in the northeastern portion of the project area. Petrological and geochemical work on these volcanic rocks and associated clastic and chemical metasedimentary rocks is the focus of M.Sc. research by the senior author at the University of Saskatchewan. This study is being integrated with other ongoing research to establish and calibrate the geological evolution of Cumberland Peninsula.

The ultramafic volcanic rocks exposed on Totnes Road Fiord are distinguished from the majority of ultramafic volcanic rocks worldwide in that they display a variety of primary fragmental textures and exhibit Ti and HFSE enrichment. Currently, the Totnes Road volcanic rocks are believed to be the older of two Paleoproterozoic mafic-ultramafic volcanic units on Cumberland Peninsula. Ongoing research will result in better stratigraphic, textural, and geochemical constraints for all metavolcanic rocks on the peninsula to help determine the volcanological and petrogenetic evolution of these rocks. Elsewhere in the region, mafic and/or ultramafic volcanic rocks occur in the Bravo Lake Formation of the Piling Group exposed on central Baffin Island (Johns et al., 2006) and in the Schooner Harbour sequence exposed on southwest Baffin Island (Sanborn-Barrie et al., 2008).

## REGIONAL GEOLOGY

Prior to this GEM initiative, the bedrock geology of Cumberland Peninsula was mapped at a reconnaissance (1:1 000 000) scale (Jackson and Taylor, 1972) and only a regional compilation of that mapping was published (St-Onge et al., 2006a). The rocks were described as a "thick succession of intensely deformed, layered metasedimentary rocks and intermediate to basic metavolcanic rock," and were designated the Hoare Bay group. With only this reconnaissance data, the regional geological context of Cumberland Peninsula has remained elusive. Cumberland Peninsula is situated between the Archean Rae Craton to the northwest and the Meta Incognita micro-continent to the south (Fig. 1). It is thought that these two terranes collided during the Foxe Orogen, one of several collisional events that collectively define the Trans-Hudson Orogen (St-Onge et al., 2006b). This collision is purported to have occurred between 1.88 and 1.865 Ga (St-Onge et al., 2006b) and is thought to be demarcated by the Baffin Suture (Fig. 1). Due to a lack of constraints in this frontier region, the regional geological context of the area was unknown and regional correlations tentative. St-Onge et al. (2009) correlated the Hoare Bay

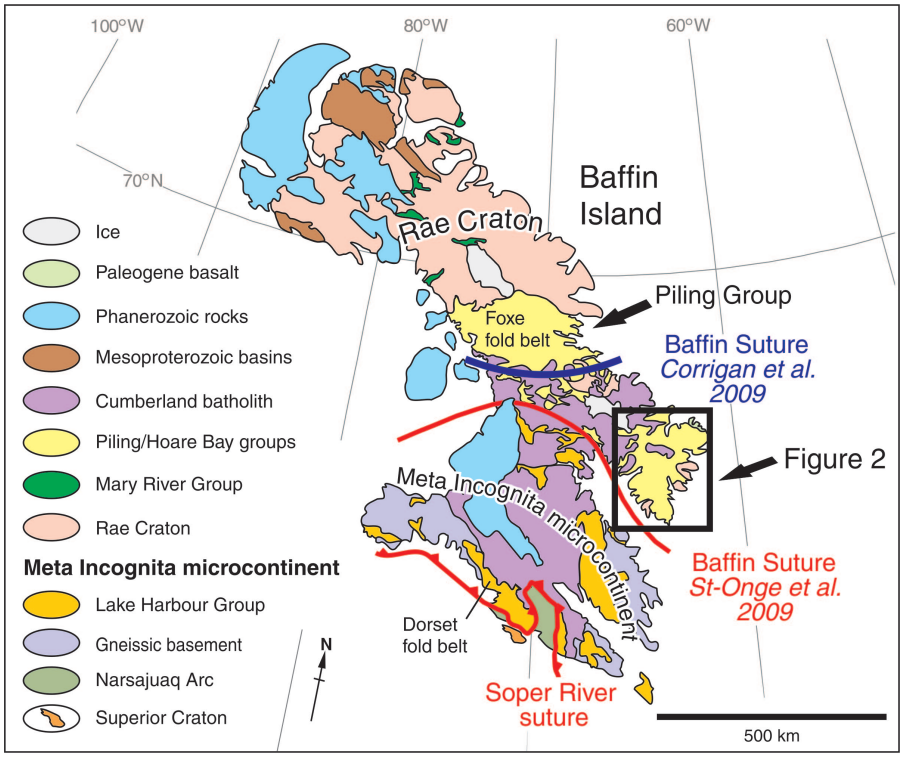


**Figure 1.** Geological map of Baffin Island showing location of Piling, Hoare Bay, and Lake Harbour Groups. The possible locations of the Baffin Suture according to Corrigan et al., (2009) and St-Onge et al. (2009) are shown. The black box outlines the area shown in Figure 2, which is the location of the Cumberland Peninsula Integrated Geoscience (GPIG) project. Map *modified from* Smye et al. (2009).

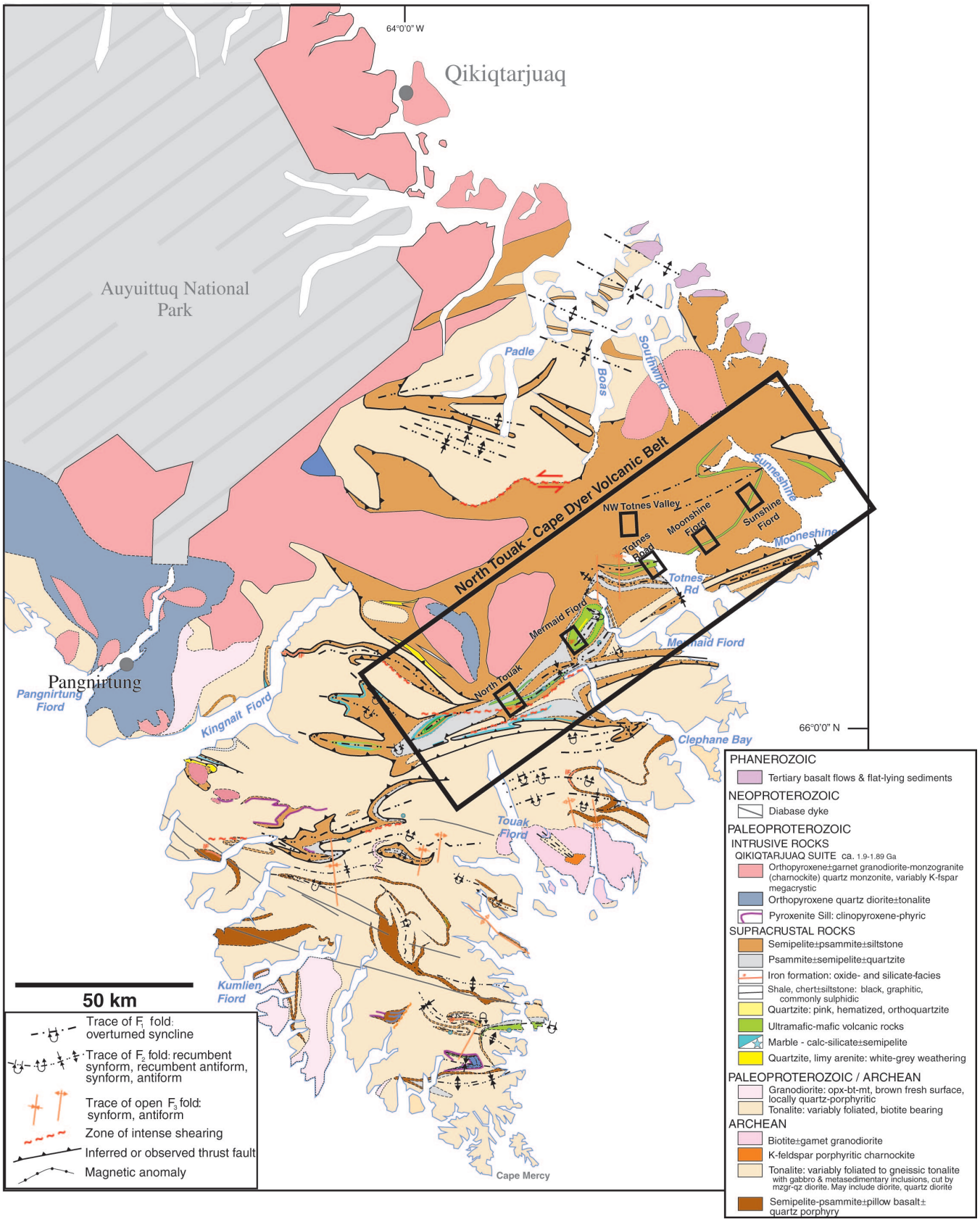


**Figure 2.** Map of the Cumberland Peninsula after bedrock mapping in summers of 2009 and 2010. Note the occurrence of mafic/ultramafic volcanic rocks (green) in the east and marbles (blue) to the west. Large black rectangle outlines the volcanic belt found on Cumberland Peninsula; small rectangles outline the areas covered during relevant foot traverses by the senior author. Map *annotated from* Sanborn-Barrie et al., (2010).

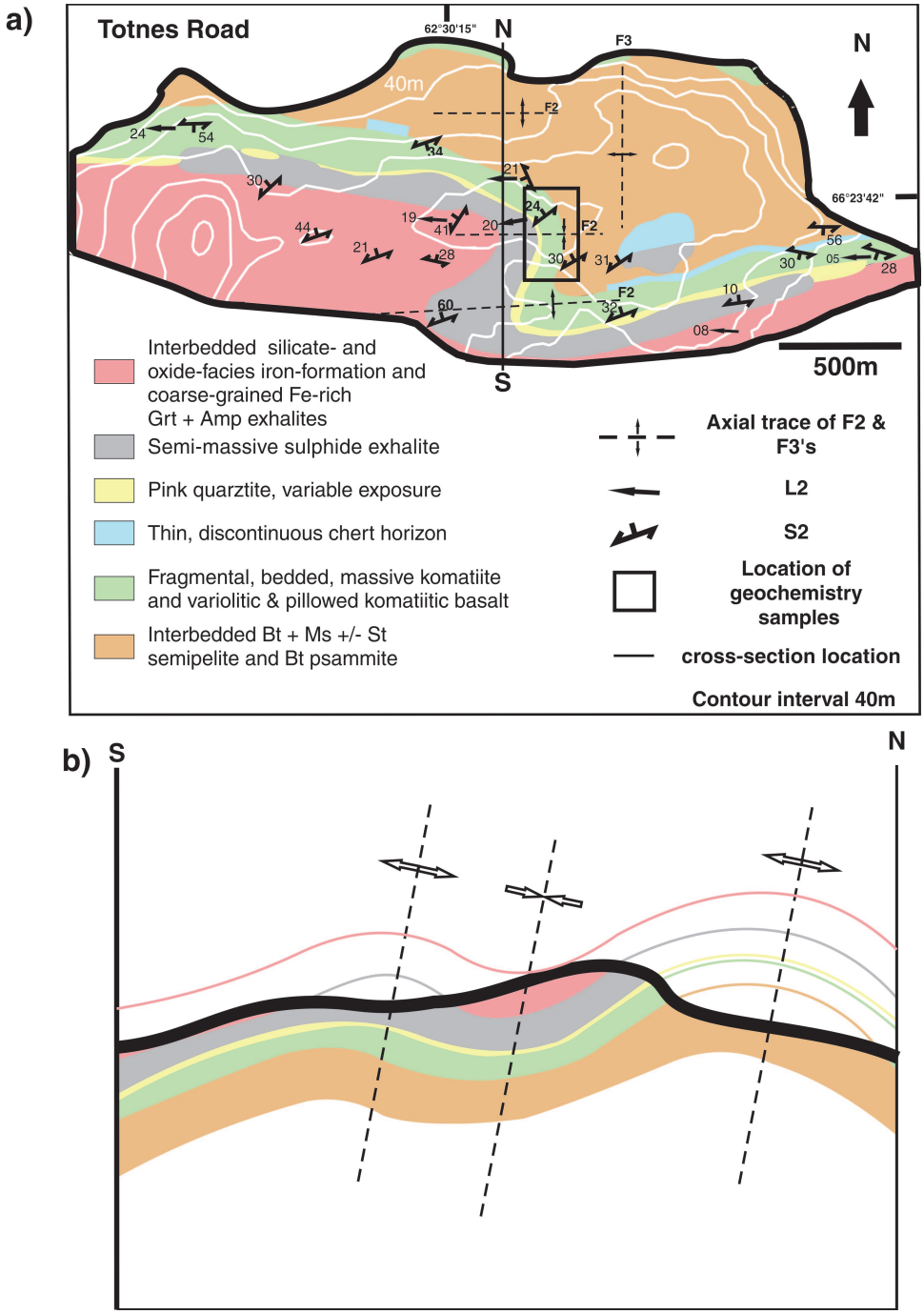


**Figure 3. a)** Geological map of the peninsula on the south shore of Totnes Road Fiord. Abbreviations: Grt – garnet, Amp – amphiboles, Bt – biotite, Ms – muscovite, St – staurolite. **b)** north-south cross-section constructed perpendicular to $F_2$ fold axes and showing the open and slightly inclined geometry of $F_2$ folds. *See* Figure 3a for location.

group to the Piling Group exposed on central Baffin Island, a Paleoproterozoic supracrustal sequence deposited on the Rae Craton, and thus placed the Baffin Suture to the south of the Cumberland Peninsula. In contrast, Corrigan et al., (2009) suggested that the Hoare Bay group may not have been deposited on the Rae Craton (Corrigan et al., 2001) and tentatively placed the Baffin Suture to the north of the Cumberland Peninsula. One of the goals of the Cumberland Peninsula project is to resolve the tectonic significance of the Hoare Bay group.

In stark contrast to earlier mapping, 1:200 000 scale mapping during the present study has revealed vast expanses of Archean plutonic and lesser supracrustal rocks, in tectonic contact with Paleoproterozoic supracrustal rocks (Sanborn-Barrie et al., 2010; 2011). At least two strongly penetrative deformation events have affected all of the rocks on Cumberland Peninsula resulting in transposed and commonly tightly infolded contacts between the Archean crystalline basement rocks and the overlying Paleoproterozoic supracrustal rocks. Although supracrustal rocks of Archean age have now been established on southern Cumberland Peninsula (N. Rayner, unpub. data, 2010; N. Wodicka, unpub. data, 2010), the volcanosedimentary sequence highlighted herein is believed to be Paleoproterozoic, possibly deposited at a similar time as the Piling Group of central Baffin (Scott et al., 2002) and Lake Harbour Group of southern Baffin (Sanborn-Barrie et al., 2008). Recent mapping suggests that Paleoproterozoic cover rocks of the Hoare Bay group are much more restricted than first interpreted (Jackson and Taylor, 1972). They comprise marble and quartzite in the west and thick successions of clastic rocks with associated metavolcanic rocks and chemical metasedimentary rocks in the east: a geographic distribution suggestive of a shallow shelf depositional environment in the west and a deeper basinal environment in the east (Fig. 2).

## GEOLOGY OF TOTNES ROAD MAP AREA

Detailed mapping of the shores of Totnes Road Fiord, in the northeastern part of the map area (Fig. 2) has revealed a spectacular section of ultramafic metavolcanic and associated metasedimentary rocks. The exposure and preservation of the above-mentioned section at Totnes Road is superior to any other location on Cumberland Peninsula where these lithologies are located. Thus, it would seem to be warranted to refer to Totnes Road as the type locality for the ultramafic metavolcanic rocks and the metasedimentary rocks associated with them. At Totnes Road three main lithological units were identified (Fig. 3). From east to west, these include 1) fine-grained, grey biotite-muscovite±staurolite, ±garnet semipelite and psammite; 2) fragmental, pillowed and massive komatiitic volcanic rocks; and 3) chemical metasedimentary rocks including sulphide-rich graphitic shale, chert, silicate and oxide-facies iron-formation, and sulphidic exhalites. A thin, <2 m thick, discontinuous quartzite unit is found in direct contact above the metavolcanic rocks at certain locations on the Totnes Road peninsula, but is absent, either due to depositional or preservation differences, at other locations. Detrital zircons from this quartzite yield a dominant population with a mean age of ca. 2 Ga (N. Wodicka, unpub. data, 2011) indicating the sedimentary sequence and associated volcanic rocks are Paleoproterozoic. This paper presents a preliminary, largely field-based examination of the komatiitic rocks supported by select geochemical analyses, and will be expanded through ongoing M.Sc. research.

The komatiitic suite at Totnes Road weathers a distinctive bright green and can be subdivided into eight separate subunits based primarily on textural differences observed in the field (Fig. 4). Deformation has resulted in the development of a strong stretching lineation and weak to moderate

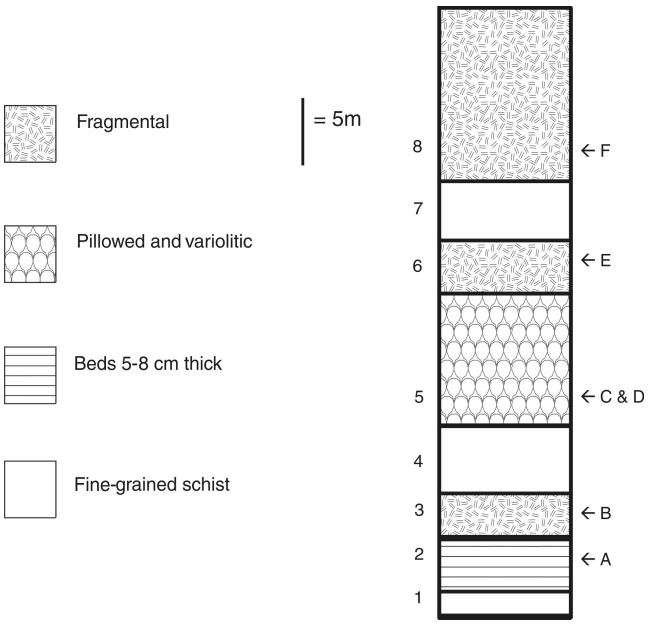


**Figure 4.** Stratigraphic column through the komatiitic unit on Totnes Road Fiord. Arrows with letters correspond to location where field pictures in Figure 5 where taken. The unit numbers 1 to 8 are located at the base of the unit in the column. *See* text for discussion of stratigraphic younging direction.

planar fabric with domains of intense shearing. Primary textures are well preserved perpendicular to the lineation and moderately well preserved in other planes. These textures are used to define the eight subunits and are listed in stratigraphic order: 1) schistose, 2) bedded, 3) fragmental, 4) schistose, 5) pillowed and variolitic, 6) fragmental, 7) schistose, and 8) fragmental. Notably absent in the Totnes Road section is spinifex texture, a reflection of ultra-rapid cooling (quenching) which is diagnostic of most komatiites. The volcanic succession is interpreted to young in a westerly direction due to the presence of accessory fragments in the more westerly unit 6 which contain varioles from unit 5.

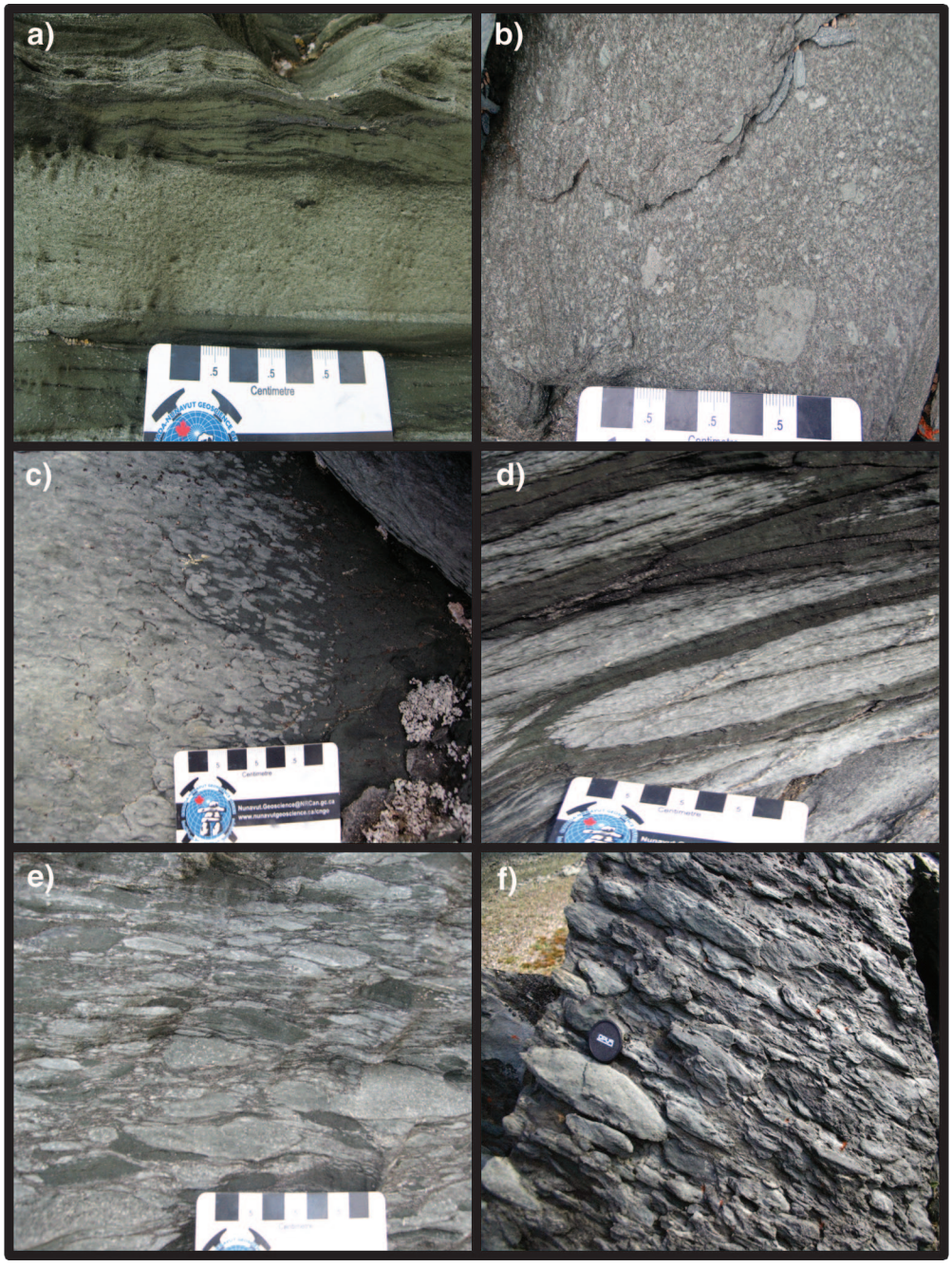


**Figure 5.** Textures preserved in komatiites at Totnes Road Fiord. **a)** Bedded tuff. 2011–036. **b)** Lapilli stone showing fragmental nature on smaller scale; taken down plunge of $L_2$. 2011-037. **c)** Varioles coalescing to cover entire outcrop surface. 2011-038. **d)** Pillow selvages with varioles concentrated in centres of individual pillows. 2011-039. **e)** Pyroclastic breccia with some variolitic fragments. 2011-040. **f)** Pyroclastic breccia highlighting highly fragmental nature of the komatiites, lens cap for scale. 2011-041. *See* Figure 4 for location of photographs.

Based upon our preliminary understanding of the structure of Totnes Road, the stratigraphically lowest unit of the komatiitic succession (unit 1) is 2 m thick, medium grained, and gossanous. Unit 2 is characterized by layering, 5 to 8 cm thick, (Fig. 5a) interpreted to represent bedding. Unit 3 displays distinct fragments (Fig. 5b) evident by grain size, mineralogical variations, and alteration differences. Throughout unit 3, fragments range from 5 mm to approximately 10 cm and vary from angular to well rounded, consistent with a tuff breccia. Tectonic alignment of fragments and stretching parallel to regional $L_2$ defines a strong L>S fabric in this unit. Unit 4 is a fine-grained schist with no visible bedding or fragments. Pillowed and variolitic unit 5 (Fig. 5c, 5d) occurs in the central portion of the volcanic package. This unit weathers black-green, rather than the more typical bright green, suggesting that this central package may be more basaltic in composition. Varioles, or ocelli, 1 cm long, occur as elliptical patches that are plagioclase-rich and hence more leucocratic than the host komatiite or komatiitic basalt (Gélinas et al., 1976; Fowler et al., 1987; Fowler et al., 2002). In unit 5, the varioles are most concentrated in the core of each pillow, where they coalesce such that the weathered colour of the rocks changes from dark black-green to light grey (Fig. 5d). The origin of varioles is still enigmatic, with interpretations including alteration, metamorphism, liquid immiscibility, processes during chilling (Arndt and Nisbet, 1982), and mingling between basalt and rhyolite (Fowler et al., 2002); however, the most likely explanation is that they are the result of spherulitic crystallization due to undercooling of the liquid (Gélinas et al., 1976). Unit 6, a tuff breccia, is similar to unit 3, except that unit 6 contains fragments with varioles (Fig. 5e) which, if derived from unit 5, suggest the sequence youngs to the west. Unit 7 is a fine-grained schist, similar to unit 4. The uppermost unit is a clast-supported pyroclastic breccia (Fig. 5f) with the largest (up to 20 cm) and most rounded fragments of the entire sequence.

Mineralogical differences between the units are minimal, with all units dominated by amphibole, primarily strongly pleochroic green magnesiohornblende, with smaller amounts of pale, weakly pleochroic amphibole, possibly ferrohornblende or actinolite. Minor mineral phases include chlorite, ilmenite with exsolved magnetite, and secondary carbonate. Plagioclase is the dominant mineral in the varioles. This mineral assemblage suggests that the rocks currently preserve amphibolite facies, having undergone complete recrystallization of the original magmatic pyroxenes and olivine.

The Totnes Road area records evidence of two penetrative deformation events, which are similar in timing, geometry, and finite strain to those observed in other parts of Cumberland Peninsula. Throughout the Cumberland Peninsula, rocks display strong $S_1 \pm S_0$ fabrics, which are tightly to isoclinally folded ($F_2$) and a strong, west-plunging $L_2 \pm L_1$ lineation. Open $F_3$ folds result in variability in the trend of the $L_2$ as well as warping the limbs of the $F_2$ folds. In the Totnes Road locality, $F_2$ folding has resulted in 200 m to 500 m scale, open folds of a strong bedding-parallel fabric (Fig. 3a and 3b). Tight to isoclinal parasitic folds occur on the limbs of the $F_2$ folds. A strong, moderately west-plunging $L_2$ lineation is developed throughout the area consistent with regional trends. A broad, open north-trending $F_3$ fold affects Totnes Road rocks by warping the limbs of the $F_2$ folds and slightly reorienting the $L_2$ lineation.

## OTHER OCCURRENCES OF VOLCANIC-BEARING SUPRACRUSTAL SEQUENCES ON CUMBERLAND PENINSULA

Foot traverses in other parts of Cumberland Peninsula (Fig. 2), allowed examination of other volcanic-bearing supracrustal sequences. Two locations, Moonshine Fiord to the northeast and Mermaid Fiord to the southwest, exposed ultramafic to mafic metavolcanic rocks and chemical metasedimentary rocks (Fig. 6). Detailed mapping of these localities was undertaken in order to compare these sections to the 'type' Totnes Road section.

At both locations, fragmental, mafic black-green weathering metavolcanic rocks are interstratified with bright-green weathering, and thus potentially ultramafic, rocks. Varioles and pillows were not observed at either location. In contact with the volcanic rocks at both locations are chemical sedimentary rocks in the form of banded oxide and silicate-facies iron-formation (Fig. 7e), as well as sulphide-rich exhalites (Fig. 7c). Clastic sedimentary rocks are abundant at both localities and consist of two distinct packages: 1) biotite-sillimanite-garnet±staurolite±muscovite-bearing semipelite to pelite (Fig. 7a), and 2) andalusite-bearing semipelite. Notably absent at both locations, in contrast to Totnes Road Fiord, is quartzite in contact with metavolcanic rocks. It is not entirely clear whether this is a result of the

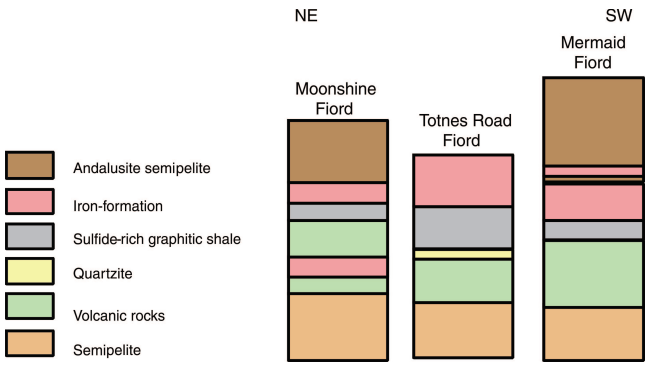


**Figure 6.** Schematic stratigraphic columns constructed at three localities that had the most complete exposure of the volcanic portion of the supracrustal sequence. *See* Figure 2 for the locations of the three sections. The general section appears to consist of semipelite, volcanic rocks, interlayered sulphides and black shale, iron-formation, semipelite. Scale is relative.

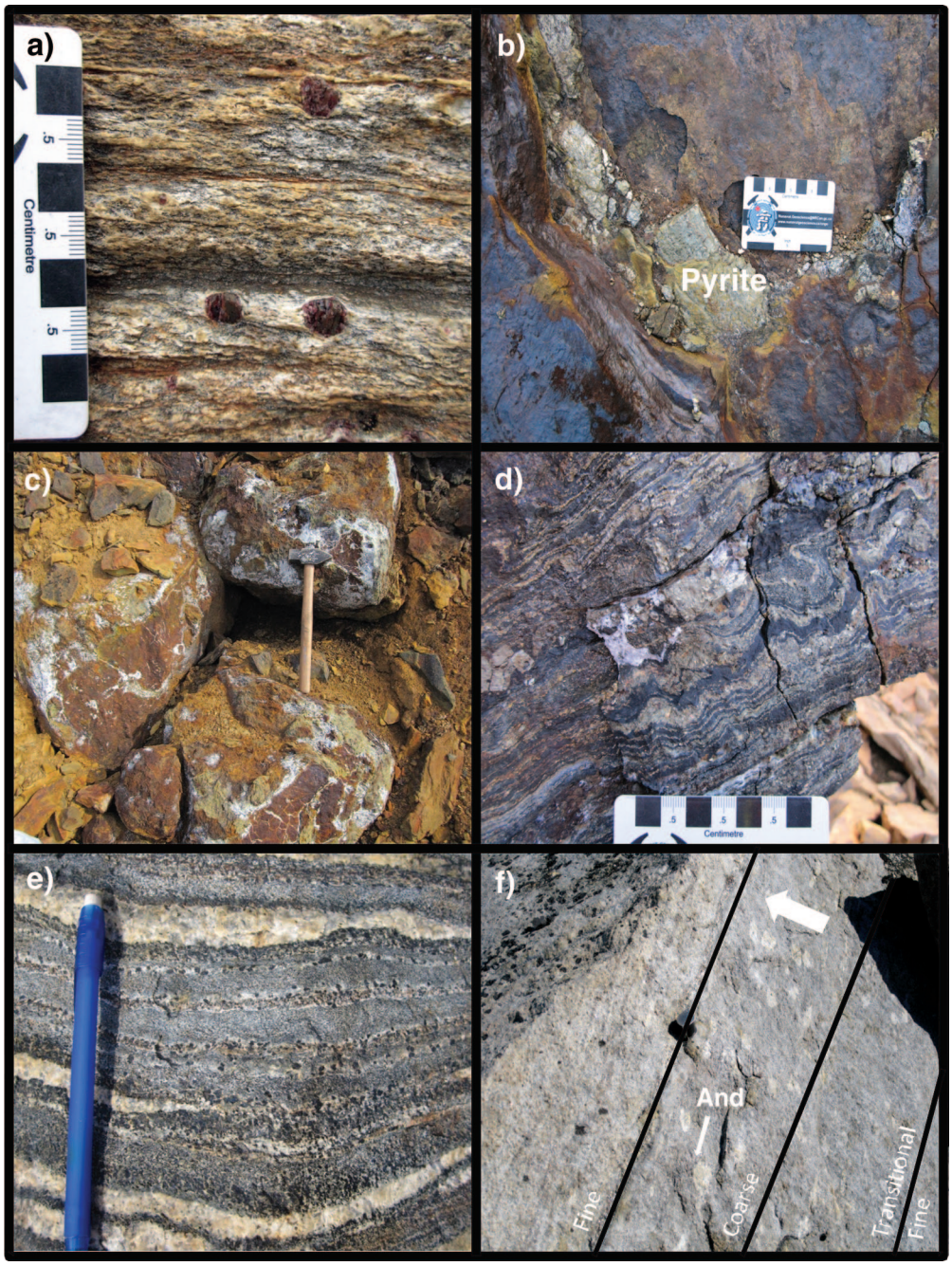


**Figure 7.** Different rock types found in the supracrustal package. **a)** Garnet-, biotite-, and sillimanite-bearing pelite from lower sediment package, northwest Totnes Valley traverse. 2011-042. **b)** Pyrite layer in graphitic black shale, Totnes Road Fiord. 2011-043. **c)** Sulphide-rich graphitic shale boulders displaying distinctive gossanous oxidation and white weathering (caliche), from northwest Totnes Valley traverse. 2011-044. **d)** Well developed $F_2$ folds folding $S_0$+$S_1$ in pyritic carbonaceous black shale, Totnes Road Fiord. 2011-045. **e)** Coarse-grained magnetite in oxide-facies iron-formation, northwest Totnes Valley traverse. 2011-046. **f)** Way-up indicator: coarsening And (andalusite) crystals in semipelite recording fining upwards sequence, arrow indicates way up, Mermaid Fiord. 2011-047

low preservation potential of this unit or lack of quartzite deposition at the Moonshine and Mermaid localities (Fig. 7b and 7d).

Stratigraphic columns constructed for exposed sections at the Moonshine and Mermaid locations (Fig. 6), allow comparison to the stratigraphy observed at Totnes Road. These stratigraphic columns are based solely on observations made in the field and the scale is relative. It was initially assumed that the volcanic rocks lie stratigraphically beneath the chemical metasedimentary rocks at the Moonshine and Mermaid localities, based on the interpreted relationships at Totnes Road Fiord. At the Mermaid Fiord locality, graded bedding in an andalusite-bearing semipelite sequence (Fig. 7f) suggests younging to the northwest, which agrees with the interpretation from Totnes Road that volcanic rocks underlie chemical metasedimentary rocks. Based on these observations, interpretations, and assumptions, the stratigraphy appears relatively consistent along a 60 km strike-length reflected by these three localities (Fig. 6). The base is interpreted to be the clastic biotite-sillimanite-garnet±staurolite ±muscovite-bearing semipelite to pelite package, overlain by mafic-ultramafic fragmental volcanic rocks, in turn overlain by chemical metasedimentary rocks and capped by andalusite-bearing semipelite.

## GEOCHEMISTRY OF TOTNES ROAD VOLCANIC ROCKS

Whole-rock major- and trace-element data for select samples (n = 13) from Totnes Road were obtained at the Ontario Geological Survey (OGS) Geoscience Laboratories. Major elements were determined by analysis of fused glass discs by X-ray fluorescence spectroscopy (XRF), FeO was determined by dichromate titration, and trace-element data were obtained using a combination of inductively coupled plasma atomic-emission spectrometry (ICP-AES) and inductively coupled plasma mass spectrometry (ICP-MS) techniques. The complete data set is shown in Table 1, and sample locations are indicated on Figures 3 and 4.

### Major-element geochemistry

Prior to interpreting geochemical data from the Totnes Road komatiite suite, it was important to assess critical factors experienced by the amphibolite-facies rocks, such as degree of element mobility and alteration. Although even unmetamorphosed komatiites have generally experienced some degree of element mobility and alteration (Arndt, 2008), it has been shown that $SiO_2$, $Al_2O_3$, $TiO_2$, FeO, MgO, and CaO, along with the REE and HFSE, are not significantly affected. Accordingly, these elements are frequently used to provide constraints on the genesis of komatiites (Beswick, 1982). To assess the degree of elemental mobility, bivariate plots (Pearce 1996) were constructed using representative immobile and mobile elements for the Totnes Road komatiites (Fig. 8). Approximately linear relationships between plotted elements such as Zr, Ti, and Ta, suggest that these elements have not been significantly affected by later alteration and metamorphic processes, whereas Rb and Ba, which show scatter when plotted against Zr, appear to have been more mobile during the same processes (Fig. 8).

The most basic geochemical definition of a komatiite is a volcanic rock with MgO >18 wt % (Arndt and Nisbet, 1982). The Totnes Road volcanic suite has MgO values ranging from 5.99 wt % to 20.27 wt % (Table 1). Units 2, 6, and 8 all have MgO values >18 wt %, clearly distinguishing them as komatiites. Units 4 and 7 have elevated MgO contents of 16.14 wt % and 15.16 wt %, respectively. Given their similar primary textures, mineralogy and weathered colour, these units are classified as basaltic komatiites, meaning they have only slightly <18 wt % MgO. Komatiitic basalts are any volcanic rock that has much less than 18 wt % MgO but can be linked by petrography, texture, or geochemistry to komatiites (Arndt, 2008). Unit 5 can thus be considered a komatiitic basalt, with its MgO contents of 5.99 to 9.10 wt % and high concentrations of Cr and Ni (comparable to the komatiitic units) in both the variolitic and non-variolitic sections.

Subdivision of komatiites on the basis of alumina was proposed by Nesbit et al. (1979), given the observation that alumina values varied among komatiites worldwide and the understanding that alumina content is controlled by the depth of the melt source. Alumina-undepleted komatiites (AUK) were first described in Munro Township in the Abitibi greenstone belt of Canada (Pyke et al., 1973) and characterized by chondritic ratios of $CaO/Al_2O_3$ (~1) and $Al_2O_3$ / $TiO_2$ (~20), with flat REE patterns (Nesbit et al., 1979). Alumina-depleted komatiites (ADK) were first described from the Barberton greenstone belt in South Africa (Viljoen and Viljoen, 1969), and characterized by higher $CaO/Al_2O_3$ around 1.5, much lower $Al_2O_3$ / $TiO_2$ of approximately 11, and HREE depletion (Nesbit et al., 1979). Depletion in alumina and HREEs is consistent with majorite garnet being present in the residue during melting. Garnet is only stable in the mantle at depths of >250 km, therefore ADK reflect deep-mantle melting, whereas AUK reflect relatively shallow melting. The Totnes Road komatiitic suite has an average $CaO/Al_2O_3$ of 1.22, an average $Al_2O_3$ / $TiO_2$ of 8.64, and is depleted in HREEs relative to LREEs, although all REEs are enriched relative to primitive mantle (Fig. 9). As such, the Totnes komatiitic suite would appear to fall within the alumina depleted classification of Nesbit et al. (1979).

However, a distinctive geochemical aspect of the Totnes Road komatiitic suite is its unusually high concentrations of $TiO_2$ (Fig. 10a), which range between 0.83 and 1.80% (Table 2). In contrast, AUK and ADK typically contain 0.3 to 0.4 wt % $TiO_2$ (Viljoen et al., 1983 and Xie et al., 1993). Although there is no strict definition of Ti enrichment in komatiites, an examination of available literature suggests that komatiites with >0.5% $TiO_2$ are considered enriched. Given that the Totnes Road komatiites are enriched in $TiO_2$,

it may not be appropriate to use Nesbit's classification scheme given that $TiO_2$ is used to determine Al depletion. Closer examination of Totnes $Al_2O_3$ values (5.4–11.28%) compared to Al-undepleted komatiite $Al_2O_3$ values from the Munro Township (4.3–9.6%) suggest that the Totnes Road suite is not alumina depleted (Fig. 10b).

High Ti komatiites, although rare, are described at several other localities worldwide. Those with $TiO_2$ values >0.5% and commonly >1.0% occur as part of a Paleoproterozoic succession in Finland (Barnes and Often, 1990) and French Guiana (Capdevila et al., 1999), as well as Neoarchean successions in Australia (Barley et al., 2000) and the Superior Province of Canada (Tomlinson et al., 1999). The above-mentioned Ti-enriched komatiites are similar to the Totnes Road suite in that they have a conspicuous lack of spinifex texture and are typically fragmental in nature. Although all reported Ti-enriched komatiites are interpreted as having erupted through continental crust, further investigation into geochemical signatures as well as geochronological studies will be used to determine if the Totnes Road komatiites also erupted through ancient continental crust. The wide geographic spread and strong similarities between these Ti-enriched komatiites prompted Barley et al. (2000) to propose a new komatiite subtype named after the belt from which they were first described, the Karasjok greenstone belt of Finland (Barnes and Often, 1990).

## Trace-element geochemistry

All komatiite varieties are generally enriched in incompatible trace elements, specifically the HFSE (particularly Th, Nb, Ce, Hf, Zr, Ti, and Y (Nesbit et al., 1979)), compared to primitive mantle (Sun and McDonough, 1989). Karasjok-type komatiites display the most enrichment, ADK display moderate enrichment, and AUK display depletion for some elements and only slight enrichment for others

**Table 1.** Whole-rock analyses for the Totnes Road Komatiites.

| Sample Name | R097C | R097C-1 | R097-C2 | R097E-1 | R097F-4 | R097F1-0 | R097F1-1 | M105A-1 | M105A-2 | R098B-2 | R098B-3 | R098B-4 | R098B-5 |
|---|---|---|---|---|---|---|---|---|---|---|---|---|---|
| Unit | 2 | 2 | 2 | 4 | 5 | 5 | 5 | 6 | 6 | 7 | 8 | 8 | 8 |
| *(wt%)* | | | | | | | | | | | | | |
| $SiO_2$ | 44.79 | 44.17 | 45.99 | 44.53 | 53.03 | 48.57 | 51.20 | 43.12 | 43.14 | 47.20 | 43.44 | 49.03 | 45.29 |
| $TiO_2$ | 1.24 | 1.35 | 0.97 | 1.63 | 1.36 | 1.80 | 1.44 | 1.01 | 0.95 | 0.83 | 0.89 | 1.05 | 0.84 |
| $Al_2O_3$ | 8.71 | 9.26 | 11.28 | 8.36 | 10.55 | 9.86 | 11.38 | 11.06 | 9.39 | 8.10 | 8.66 | 5.41 | 8.60 |
| $Fe_2O_3$ | 2.19 | 2.21 | 2.26 | 5.48 | 8.05 | 7.01 | 7.11 | 3.73 | 2.05 | 1.90 | 1.77 | 1.59 | 2.36 |
| FeO | 10.18 | 10.66 | 9.28 | 8.87 | 7.73 | 9.75 | 7.92 | 10.29 | 9.51 | 8.37 | 9.34 | 8.40 | 8.73 |
| MnO | 0.15 | 0.15 | 0.20 | 0.17 | 0.12 | 0.17 | 0.14 | 0.29 | 0.17 | 0.21 | 0.18 | 0.20 | 0.19 |
| MgO | 17.94 | 17.47 | 14.43 | 16.14 | 5.99 | 9.10 | 7.26 | 15.66 | 20.27 | 15.16 | 20.03 | 18.03 | 20.25 |
| CaO | 9.27 | 9.15 | 11.90 | 11.45 | 7.23 | 7.80 | 7.48 | 10.33 | 7.87 | 13.76 | 9.13 | 12.14 | 8.56 |
| $Na_2O$ | 0.61 | 0.69 | 1.42 | 0.97 | 5.06 | 3.42 | 4.62 | 1.57 | 0.49 | 1.33 | 0.52 | 0.85 | 0.55 |
| $K_2O$ | 0.53 | 0.57 | 0.15 | 0.15 | 0.09 | 0.68 | 0.28 | 0.13 | 0.04 | 0.09 | 0.07 | 0.10 | 0.06 |
| $P_2O_5$ | 0.12 | 0.14 | 0.08 | 0.13 | 0.17 | 0.13 | 0.17 | 0.06 | 0.07 | 0.04 | 0.06 | 0.04 | 0.06 |
| LOI | 3.45 | 3.18 | 0.77 | 1.25 | 0.09 | 0.13 | -0.04 | 2.08 | 4.97 | 2.03 | 5.20 | 2.84 | 4.11 |
| Total | 99.18 | 99.00 | 98.73 | 99.13 | 99.47 | 98.42 | 98.96 | 99.33 | 98.92 | 99.02 | 99.29 | 99.68 | 99.60 |
| $CaO/Al_2O_3$ | 1.06 | 0.99 | 1.05 | 1.37 | 0.69 | 0.79 | 0.66 | 0.93 | 0.84 | 1.70 | 1.05 | 2.24 | 1.00 |
| $Al_2O_3/TiO_2$ | 7.02 | 6.86 | 11.63 | 5.13 | 7.76 | 5.48 | 7.90 | 10.95 | 9.88 | 9.76 | 9.73 | 5.15 | 10.24 |
| *(ppm)* | | | | | | | | | | | | | |
| Cr | 1903 | 1464 | 2009 | 1533 | 1354 | 1639 | 1323 | 1869 | 2206 | 1697 | 2144 | 1061 | 2192 |
| Ni | 909.00 | 596.50 | 640.10 | 1046.20 | 426.30 | 860.50 | 457.70 | 690.20 | 1141.30 | 757.10 | 1139.20 | 703.10 | 1121.60 |
| Co | 86.43 | 83.07 | 75.09 | 98.30 | 55.76 | 117.40 | 85.53 | 84.97 | 94.97 | 83.73 | 95.79 | 77.27 | 92.49 |
| Sc | 44.40 | 30.50 | 37.00 | 32.00 | 26.60 | 36.30 | 27.60 | 39.70 | 33.40 | 33.60 | 36.70 | 32.50 | 33.60 |
| V | 318.00 | 290.90 | 286.60 | 310.70 | 325.70 | 364.60 | 319.30 | 294.20 | 262.10 | 298.30 | 282.70 | 269.30 | 280.50 |
| Cu | 848.70 | 228.50 | 63.70 | 73.50 | 68.90 | 159.20 | 81.80 | 70.30 | 109.50 | 9.60 | 88.50 | 46.20 | 177.10 |
| Pb | 1.10 | 1.30 | 0.80 | 0.60 | 1.80 | 1.80 | 2.60 | 0.80 | 0.90 | 1.30 | 1.10 | 1.30 | 0.70 |
| Zn | 95 | 98 | 79 | 104 | 84 | 124 | 95 | 87 | 81 | 85 | 79 | 74 | 79 |
| Cd | 0.11 | 0.08 | 0.08 | 0.12 | 0.09 | 0.11 | 0.08 | 0.14 | 0.12 | 0.12 | 0.09 | 0.39 | 0.12 |
| In | 0.05 | 0.06 | 0.06 | 0.06 | 0.06 | 0.08 | 0.06 | 0.06 | 0.04 | 0.06 | 0.04 | 0.05 | 0.04 |
| Sn | 1.00 | 1.34 | 0.74 | 1.07 | 1.03 | 1.15 | 1.15 | 0.66 | 0.60 | 0.82 | 0.70 | 0.71 | 0.54 |
| W | 0.12 | 0.15 | 0.11 | 0.12 | 0.12 | 0.11 | 0.12 | 0.25 | 0.14 | 0.12 | 0.09 | 0.12 | 0.08 |
| Mo | 1.29 | 0.98 | 0.31 | 0.19 | 0.12 | | 0.13 | 0.63 | 0.12 | 0.18 | 0.10 | 0.24 | |
| Sb | 0.24 | 0.23 | 0.36 | 0.22 | 0.36 | 0.16 | 0.20 | 0.21 | 0.44 | 0.20 | 0.31 | 0.52 | 0.25 |
| Rb | 14.88 | 16.75 | 1.76 | 0.54 | 0.30 | 13.68 | 4.00 | 0.36 | 0.31 | 0.52 | 1.20 | 1.53 | 0.66 |

LOI, loss of ignition. Cn, chondrite normalized. Mn, mantle normalized.

(Fig. 11). The greater amount of enrichment in the Karasjok-type komatiites (up to twice the ADK and AUK values) is a distinguishing characteristic and should be considered when defining this unusual rock type. Surprisingly, the komatiites from the type locality in Finland show the least amount of enrichment for the Karasjok-type komatiites, but they are still slightly enriched in most of the elements compared to AUK and ADK.

Karasjok-type komatiites, including those from the Totnes Road area, display distinct REE patterns. As a group, Karasjok-type komatiites display REE enrichment relative to primitive mantle. All localities, except Finland clearly show enrichment in the LREEs over the HREEs (Fig. 12) with average $La/Yb_{mn}$ values between 1.91 and 4.46 (Totnes Road = 2.87). This distinct pattern is diagnostic of Karasjok-type komatiites, whereas ADK show only slight enrichment of LREEs (average $La/Yb_{mn}$ 1.47) and AUK are strongly LREE depleted (average $La/Yb_{mn}$ 0.36).

# DISCUSSION

The Totnes Road komatiite suite, which can be classified as a Karasjok-type komatiite suite, is characterized by unusual textural (fragmental) and chemical (Ti and HFSE enrichment) characteristics that require careful integration when considering their petrogenesis.

The fragmental character of the Totnes Road komatiite suite is distinctive and somewhat unusual, given that komatiites usually erupt at such high temperatures and with such low viscosities that they tend to form thin flows (Arndt, 2008). Their fragmental nature may be explained by a process of steam explosivity — the expansion and subsequent collapse of steam formed at the magma-water interface (Kokelaar, 1986). This process may be enhanced if the komatiitic magma increased its water content on ascent through hydrated continental crust. Thus the fragmentation may be caused by a combination of steam and magmatic

**Table 1.** (Cont.)

| Sample Name | R097C | R097C-1 | R097-C2 | R097E-1 | R097F-4 | R097F1-0 | R097F1-1 | M105A-1 | M105A-2 | R098B-2 | R098B-3 | R098B-4 | R098B-5 |
|---|---|---|---|---|---|---|---|---|---|---|---|---|---|
| Unit | 2 | 2 | 2 | 4 | 5 | 5 | 5 | 6 | 6 | 7 | 8 | 8 | 8 |
| *(ppm) continued* | | | | | | | | | | | | | |
| Cs | 3.59 | 3.97 | 0.24 | 0.03 | 0.00 | 0.30 | 0.08 | 0.12 | 0.13 | 0.04 | 0.47 | 0.38 | 0.24 |
| Ba | 464.70 | 461.70 | 17.00 | 37.20 | 47.00 | 227.60 | 155.80 | 9.40 | 2.10 | 18.90 | 13.20 | 17.50 | 7.10 |
| Sr | 118.60 | 115.70 | 129.50 | 142.90 | 239.30 | 262.40 | 420.20 | 68.60 | 80.00 | 201.50 | 129.20 | 202.00 | 88.60 |
| Ga | 12.28 | 13.23 | 14.08 | 15.23 | 15.91 | 18.26 | 18.32 | 15.58 | 13.35 | 10.33 | 12.21 | 7.91 | 11.99 |
| Li | 32.50 | 33.20 | 14.60 | 13.50 | 5.30 | 22.20 | 10.80 | 32.40 | 23.50 | 9.40 | 34.10 | 9.00 | 24.90 |
| Be | 0.74 | 0.77 | 0.31 | 0.81 | 0.66 | 1.01 | 1.02 | 0.48 | 0.39 | 0.34 | 0.62 | 0.40 | 0.48 |
| Ta | 0.49 | 0.67 | 0.26 | 0.66 | 0.56 | 0.70 | 0.58 | 0.20 | 0.27 | 0.23 | 0.23 | 0.45 | 0.25 |
| Nb | 8.32 | 10.48 | 3.87 | 10.58 | 9.37 | 11.32 | 9.69 | 3.49 | 4.10 | 3.78 | 3.46 | 6.18 | 3.93 |
| Hf | 1.91 | 2.00 | 1.41 | 2.64 | 2.26 | 2.79 | 2.28 | 1.38 | 1.30 | 1.31 | 1.14 | 1.82 | 1.10 |
| Zr | 74.00 | 77.00 | 51.00 | 105.00 | 88.00 | 111.00 | 90.00 | 50.00 | 48.00 | 48.00 | 39.00 | 69.00 | 39.00 |
| Y | 9.79 | 14.67 | 14.66 | 16.57 | 17.07 | 18.50 | 18.44 | 13.96 | 12.82 | 12.73 | 11.76 | 16.34 | 11.79 |
| Th | 0.72 | 1.23 | 0.37 | 0.88 | 0.79 | 0.94 | 0.81 | 0.28 | 0.26 | 0.32 | 0.27 | 0.54 | 0.31 |
| U | 0.31 | 0.39 | 0.10 | 0.29 | 0.21 | 0.18 | 0.21 | 0.10 | 0.11 | 0.30 | 0.09 | 0.16 | 0.10 |
| La | 6.00 | 10.17 | 4.43 | 6.53 | 12.67 | 10.11 | 10.88 | 4.05 | 3.27 | 3.38 | 2.36 | 3.60 | 3.49 |
| Ce | 15.66 | 24.66 | 9.65 | 18.11 | 28.24 | 25.60 | 27.77 | 10.09 | 8.93 | 8.85 | 6.90 | 9.60 | 9.15 |
| Pr | 2.12 | 3.17 | 1.43 | 2.87 | 3.80 | 3.78 | 4.05 | 1.53 | 1.38 | 1.38 | 1.13 | 1.54 | 1.40 |
| Nd | 9.23 | 13.79 | 6.87 | 13.98 | 16.78 | 17.75 | 18.74 | 7.37 | 6.87 | 7.00 | 6.01 | 8.06 | 6.75 |
| Sm | 2.19 | 3.48 | 2.17 | 3.88 | 4.09 | 4.65 | 4.56 | 2.22 | 2.10 | 2.14 | 1.98 | 2.60 | 1.98 |
| Eu | 1.05 | 1.46 | 0.92 | 1.19 | 1.28 | 1.39 | 1.43 | 0.95 | 0.60 | 0.91 | 0.92 | 0.78 | 0.77 |
| Gd | 2.27 | 3.59 | 2.60 | 4.03 | 4.10 | 4.87 | 4.66 | 2.64 | 2.49 | 2.40 | 2.31 | 3.10 | 2.24 |
| Tb | 0.35 | 0.57 | 0.41 | 0.60 | 0.61 | 0.70 | 0.67 | 0.43 | 0.41 | 0.40 | 0.39 | 0.51 | 0.37 |
| Dy | 2.09 | 3.36 | 2.69 | 3.52 | 3.55 | 4.06 | 3.92 | 2.73 | 2.59 | 2.44 | 2.40 | 3.14 | 2.27 |
| Ho | 0.39 | 0.62 | 0.54 | 0.64 | 0.65 | 0.73 | 0.71 | 0.54 | 0.51 | 0.48 | 0.48 | 0.62 | 0.45 |
| Er | 1.05 | 1.61 | 1.56 | 1.65 | 1.71 | 1.85 | 1.82 | 1.46 | 1.40 | 1.36 | 1.29 | 1.71 | 1.27 |
| Tm | 0.15 | 0.21 | 0.22 | 0.22 | 0.22 | 0.24 | 0.23 | 0.21 | 0.19 | 0.19 | 0.18 | 0.23 | 0.17 |
| Yb | 0.93 | 1.21 | 1.45 | 1.25 | 1.27 | 1.45 | 1.33 | 1.30 | 1.16 | 1.17 | 1.06 | 1.40 | 1.08 |
| Lu | 0.13 | 0.17 | 0.23 | 0.17 | 0.17 | 0.20 | 0.19 | 0.19 | 0.16 | 0.17 | 0.15 | 0.19 | 0.15 |
| $La/Yb_{cn}$ | 4.47 | 5.81 | 2.13 | 3.61 | 6.94 | 4.85 | 5.69 | 2.15 | 1.96 | 2.00 | 1.55 | 1.79 | 2.25 |
| $La/Sm_{cn}$ | 2.74 | 2.93 | 2.04 | 1.68 | 3.10 | 2.17 | 2.38 | 1.82 | 1.56 | 1.58 | 1.19 | 1.39 | 1.76 |
| $Gd/Yb_{cn}$ | 2.02 | 2.45 | 1.49 | 2.66 | 2.68 | 2.79 | 2.91 | 1.68 | 1.78 | 1.69 | 1.81 | 1.84 | 1.72 |
| $Gd/Yb_{mn}$ | 2.02 | 2.45 | 1.49 | 2.66 | 2.68 | 2.79 | 2.91 | 1.68 | 1.78 | 1.69 | 1.81 | 1.84 | 1.72 |
| $Eu^*/Eu_{cn}$ | 0.92 | 0.90 | 0.91 | 0.95 | 0.97 | 0.90 | 0.91 | 0.92 | 0.94 | 1.09 | 1.00 | 1.04 | 0.93 |

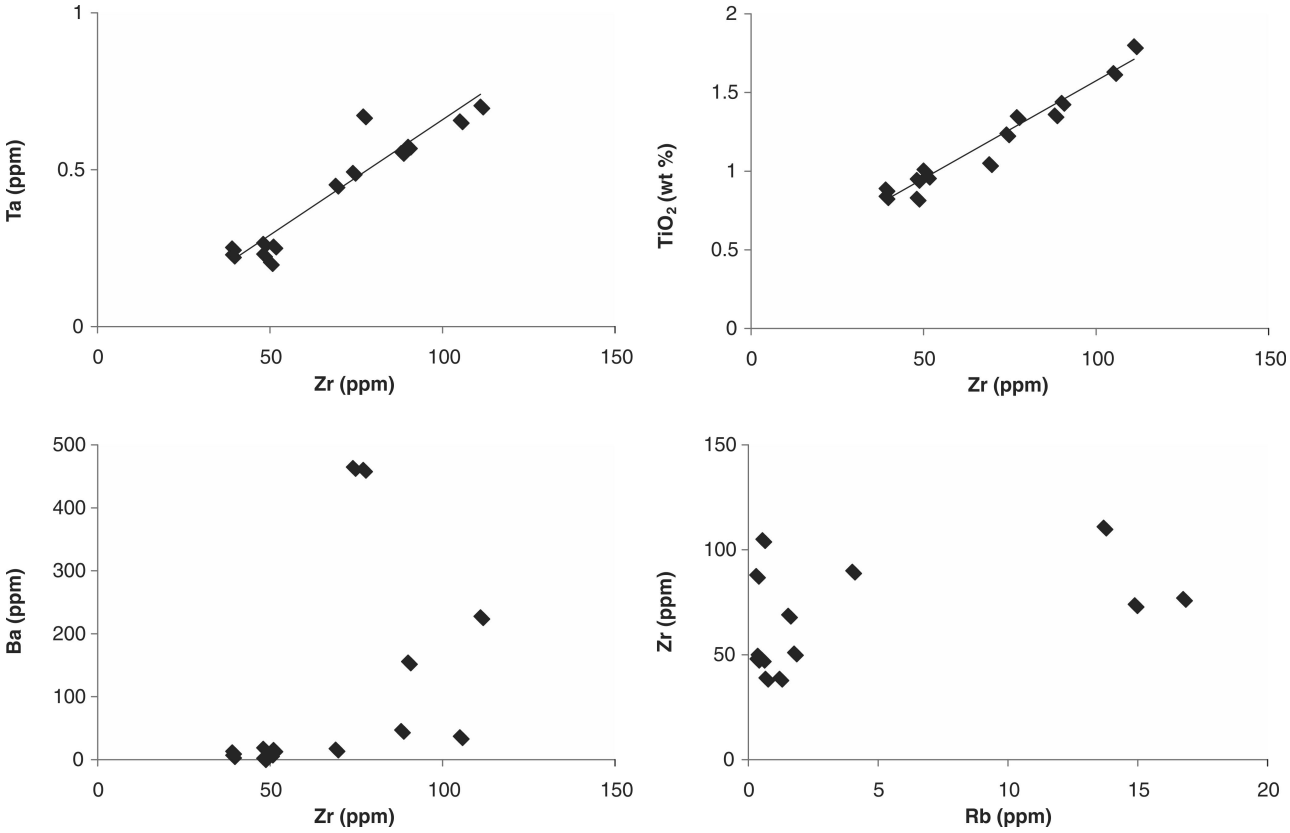


**Figure 8.** Bivariate plots of Zr versus immobile elements (Ti and Ta) and mobile elements (Rb and Ba) for Totnes Road komatiites. The immobile elements form linear arrays whereas the mobile elements exhibit a more scattered pattern.

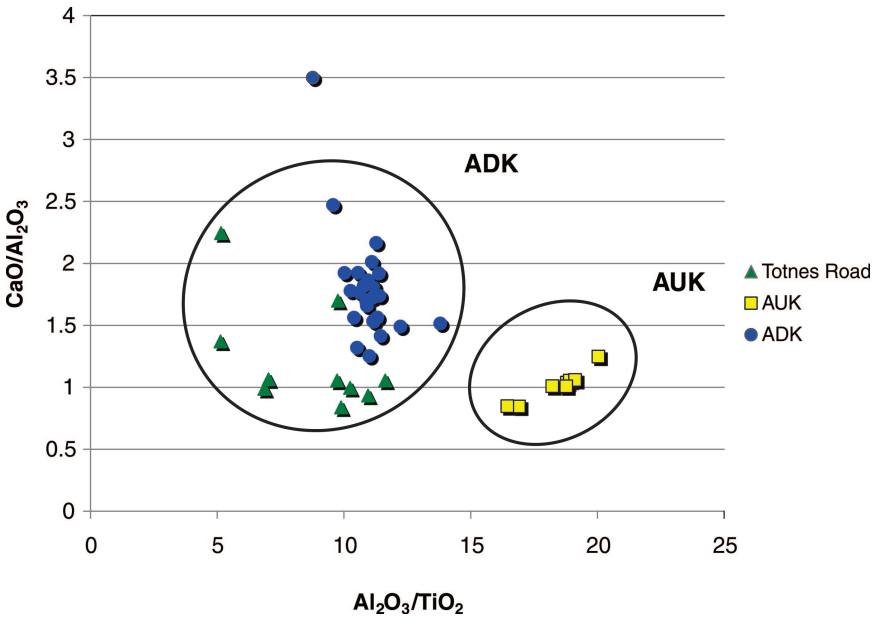


**Figure 9.** Plot of $CaO/Al_2O_3$ versus $Al_2O_3/TiO_2$ showing fields for ADK (upper left) and AUK (lower right) (*after* Nesbit et al., 1979). TRK plot within ADK field. AUK field from Munro Township (Fan and Kerrich, 1997) and ADK field from Barberton area (Viljoen et al., 1983).

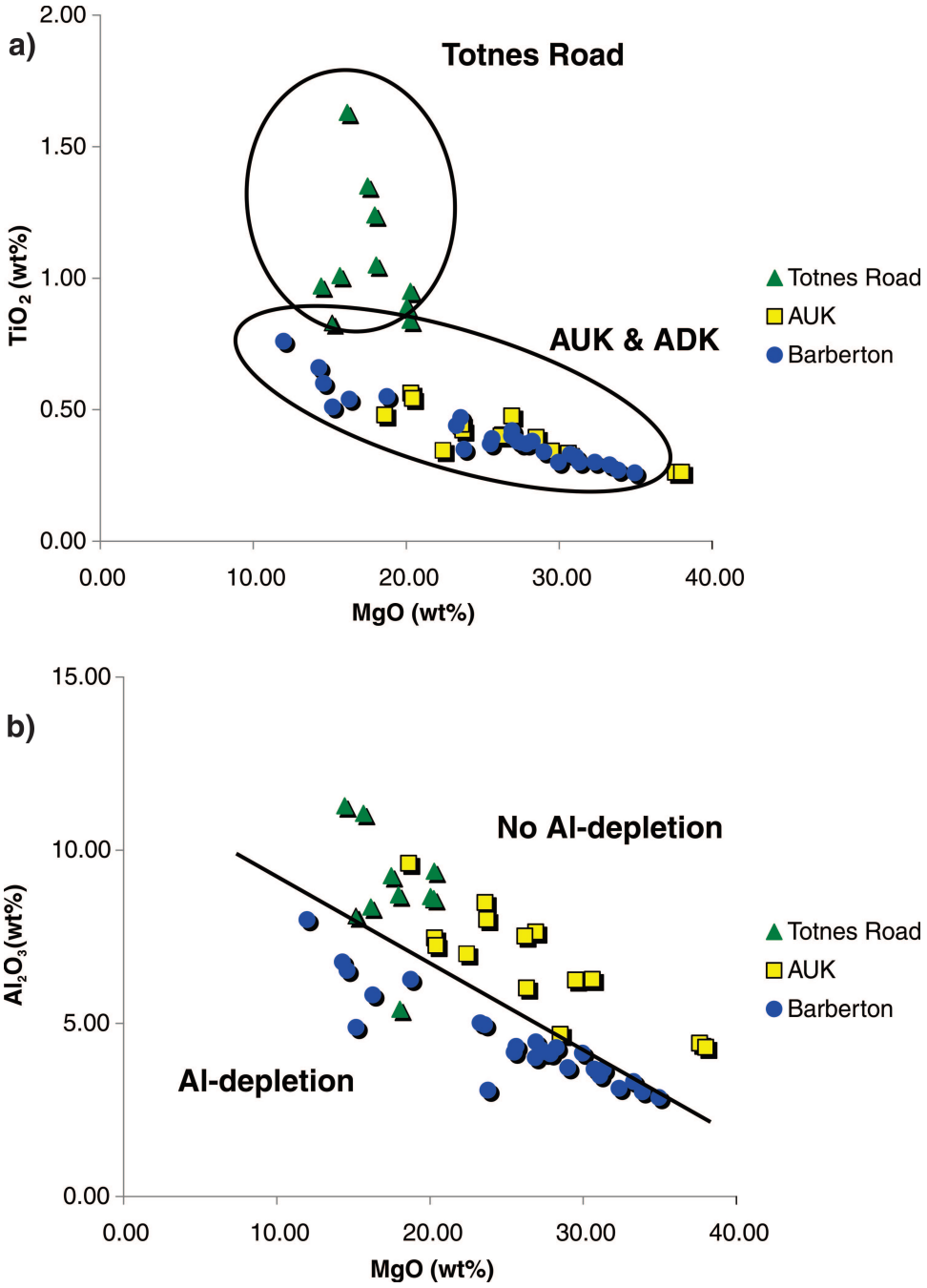


**Figure 10. a)** Plot of $TiO_2$ vs. MgO content showing the Ti-enrichment of Totnes Road komatiites as compared to AUK and ADK. **b)** Plot of $Al_2O_3$ vs. MgO showing that Totnes Road komatiites in fact are not depleted in alumina as they plot with AUK. AUK field from Munro Township (Fan and Kerrich, 1997) and ADK field from Barberton area (Viljoen et al., 1983).

explosivity, the latter being the release of magmatic volatiles upon approaching the surface (Kokelaar, 1986). All fragmentation processes are controlled by volatile content and water depth (hydrostatic pressure), and Kokelaar (1986) suggested that the maximum depth for fragmentation of mafic magmas to take place is approximately 200 m. A recent discovery on the ultraslow-spreading Gakkel ridge has shown that explosive volcanism can occur at depths as great as 4000 m; however, it was calculated that the magma would have to contain at least 13 wt % $CO_2$ in order to fragment at such high hydrostatic pressure (Sohn et al., 2008). Accordingly, all available data suggest that essentially anhydrous komatiitic magmas will fragment at shallower depths, on the order of <200 m.

Komatiitic rocks from the Totnes Road area possess distinctive geochemical characteristics which are similar to the relatively uncommon Karasjok-type komatiites. The Totnes suite is alumina undepleted, similar to komatiites from Munro Township (Fig. 10b). Depth of melting is believed to be the primary control on alumina content in komatiites, in that stability of garnet at depth sequesters alumina

**Table 2** Average whole-rock analyses for select mafic and ultramafic rock types.

| Sample | Totnes (avg) | AUK | ADK | E-MORB | N-MORB | Meimechite |
|---|---|---|---|---|---|---|
| *(wt%)* | | | | | | |
| $SiO_2$ | 45.07 | 45.98 | 45.85 | 51.2 | 50.4 | 41.21 |
| MgO | 17.54 | 28.48 | 25.53 | 1.69 | 1.36 | 33.9 |
| $TiO_2$ | 1.08 | 0.37 | 0.41 | 6.9 | 8.96 | 2.34 |
| *(ppm)* | | | | | | |
| Th | 0.52 | 0.04 | | 0.6 | 0.12 | 3 |
| Nb | 5.82 | 0.49 | 1.6 | 8.3 | 2.33 | 37.57 |
| Ce | 12.16 | 1.28 | 3.24 | 15 | 7.5 | 73 |
| Hf | 1.6 | 0.46 | 0.5 | 2.03 | 2.05 | |
| Zr | 60 | 14.95 | 30.06 | 73 | 74 | 175.67 |
| Y | 13.51 | 7.3 | 9.52 | 22 | 28 | 10.5 |

Data sources: AUK (Fan and Kerrich, 1997), ADK (Chavagnac, 2004 and Viljoen et al., 1983), E-MORB (Sun and McDonough, 1989 and Hughes, 1982), N-MORB (Sun and McDonough, 1989), and meimechite (Elkins-Tanton et al., 2006).

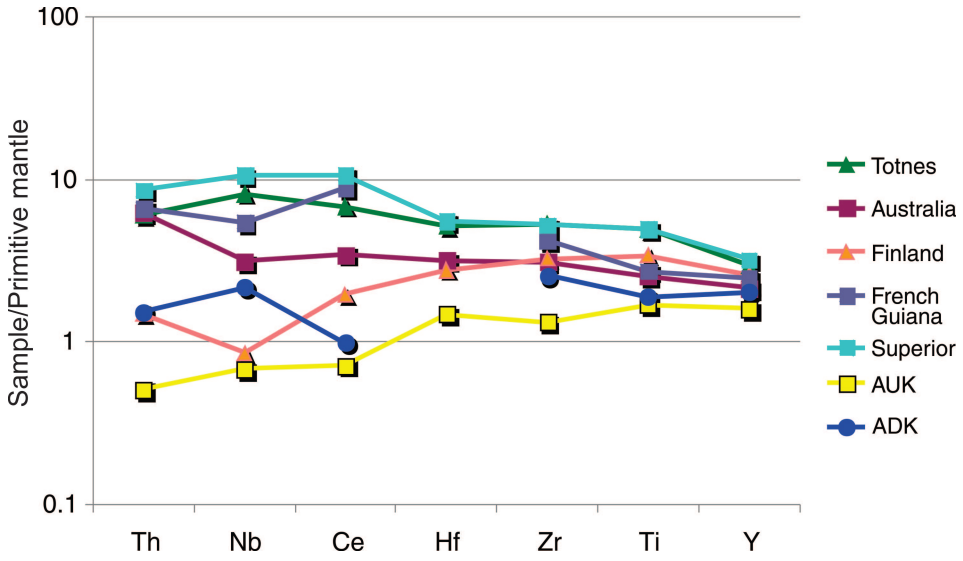


**Figure 11.** Plot of selected HFSE: Th, Nb, Ce, Hf, Zr, Ti, and Y comparing Totnes Road komatiites with other Paleoproterozoic and Archean komatiite occurrences. Komatiites from Totnes Road, Australia, French Guiana, and Superior Province are much more enriched in the HFSE than AUK and ADK. Komatiites from Finland are enriched relative to AUK and enriched relative to ADK for all elements except Th and Nb. AUK (Fan and Kerrich, 1997), ADK (Chavagnac, 2004 and Viljoen et al., 1983), and Karasjok-type komatiites from Australia (Barley et al., 2000), Finland (Hanski et al., 2001), French Guiana (Capdevila et al., 1999), and the Superior Province (Tomlinson et al., 1999). Primitive mantle values from Sun and McDonough (1989).

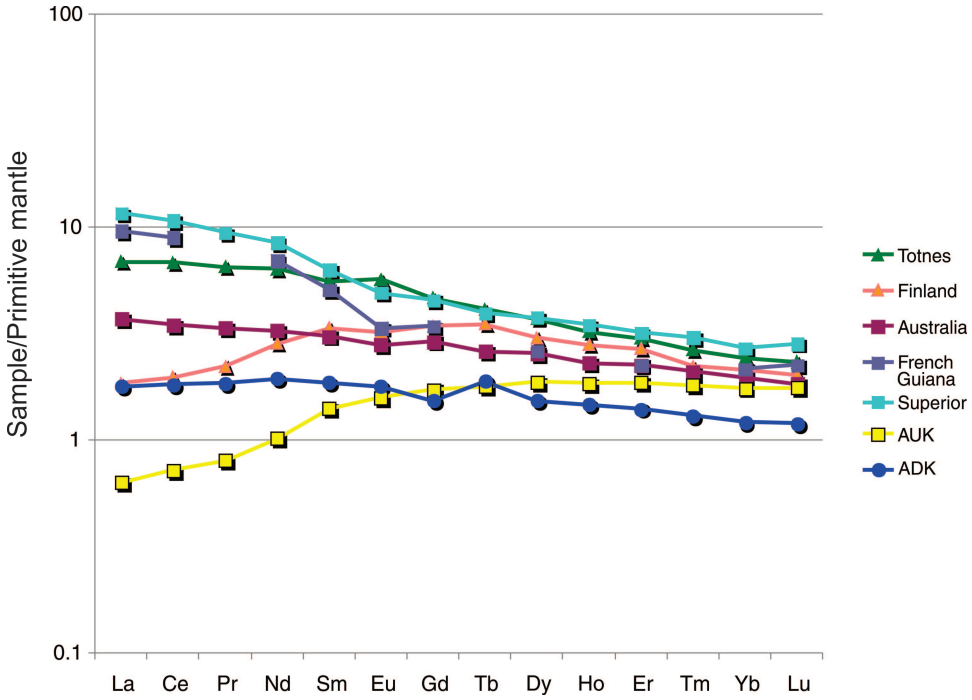


**Figure 12.** Primitive mantle (Sun and McDonough, 1989) normalized REE plot comparing Totnes Road komatiites with other Paleoproteroizoic and Archean komatiite occurrences. All komatiites, except AUK, are enriched in all the REEs. The Karasjok-type komatiites, except those from Finland, are clearly enriched in the LREEs over the HREEs. ADK have a flat, slightly LREE-enriched pattern and AUK have a characteristic LREE-depleted pattern. Referenced data as in Figure 11.

and HREEs. Alumina-undepleted komatiites (AUK) are believed to be the product of shallower melting (pressures of 5–7 GPa) since at depths <250 km, the melt will be in equilibrium with harzburgite and will not become depleted in alumina (Herzberg, 1995). Alumina-depleted komatiites (ADK) are thought to be generated at depths >250 km (pressures of 9–10 GPa, up to 14 GPa) (Herzberg, 1995), where majorite garnet is stable in the mantle. Residual garnet will result in the formation of a magma depleted in Al, HREE, and HFSE. On the basis of alumina, HFSE, and HREE content it would appear that the Totnes Road komatiites did not melt in equilibrium with garnet, consistent with their formation through melting at depths of <250 km.

A defining characteristic of the Karasjok-type komatiites, including Totnes Road, is their enrichment in the HFSEs such as Th, Nb, Hf, Zr, Ti, Y, and the LREEs compared to both AUK and ADK. Early explanations for this enrichment included alteration, contamination by continental crust, and low-pressure fractional crystallization (Barnes and Often, 1990). Recent work has shown that the most likely source of this HFSE enrichment is the mantle through which the magma ascended (Hanski et al., 2001, Capdevila et al., 1999, Gangopadhyay et al., 2005). A characteristic shared by all Karasjok-type komatiites is that they erupted through older continental, or island-arc, crustal material (Barnes and Often, 1990; Barley et al., 2000; Capdevila et al., 1999; Schaefer and Morton, 1991). The subcontinental lithospheric mantle (SCLM) beneath ancient continental blocks and island-arc systems is highly susceptible to metasomatism by both fluids and melts due to subduction processes, resulting in a geochemically fertile mantle.

Peridotite xenoliths from the SCLM show that Ti-rich minerals (rutile) that have been produced by mantle metasomatism are enriched in HFSEs (Kalfoun et al., 2002 *in* Gangopadhyay et al., 2005). Wagner and Grove (1997) have shown experimentally that Ti-oxide minerals will melt out faster than other mantle phases such as clinopyroxene (Gangopadhyay et al., 2005). Therefore if parental Al-undepleted komatiitic magma passed through fertile metasomatized SCLM, minerals enriched in Ti could be preferentially melted within the ascending magma thereby increasing its Ti and HFSE concentrations.

An alternative explanation of HFSE enrichment in Karasjok-type komatiites is through assimilation of basaltic melts by the parental magma (Gangopadhyay et al., 2005). It is assumed that the parental magma has a composition similar to AUK. If the proposed contaminating melt had a composition comparable to N-MORB or E-MORB (Sun and McDonough, 1989), the parental magma could have become enriched in Ti and other HFSEs as these basaltic

melts have much higher concentrations of both compared to Al-undepleted komatiites (Table 2). An issue with this hypothesis is that the percentage of contaminant assimilated would have to be small enough so as not to increase the $SiO_2$ content or decrease the MgO content of the parental magma, yet large enough to drastically increase the concentration of Ti and other HFSEs.

A third possibility involves retention of a small portion of the initial mantle melt. According to Arndt (2008), when mantle melts to produce an AUK, the very first batch of melt will have the composition of a meimechite. Meimechites are volcanic rocks that have extreme enrichment in the HFSEs (Table 2). It is generally thought that the initial melt is extracted from the source and the residuum melts to form an AUK parental magma (Arndt, 2008). We propose that if a small portion of initial melt was not extracted, but rather remained in the residuum, the Ti and HFSE content of the resulting parental magma would be elevated upon eruption, as in the case of Karasjok-type komatiites.

The stratigraphic association at Totnes Road, of ultramafic metavolcanic rocks, fine-grained clastic, and chemical metasedimentary rocks, suggests a basinal setting for deposition. The lowermost unit identified in the Totnes succession is a clastic semipelitic to pelitic package. Clastic sedimentation may have occurred on a rifted margin that subsequently experienced ultramafic volcanism from a deep-seated (mantle plume?) source (Herzberg, 1995). Explosive eruptions deposited fragmental, tuffaceous komatiitic material, whereas less violent eruptions resulted in komatiitic basalt and basaltic komatiite pillows and flows. High heat flow in the (plume-related?) basin was a potential catalyst for hydrothermal activity, leading to the deposition of chemical sedimentary rocks now represented by pyritic carbonaceous shale, iron formation, and local massive sulphides.

Pyritic carbonaceous shale, commonly referred to as sulphide-facies iron-formation, is believed to be deposited in slightly shallower settings than oxide-facies iron-formation. This is due to the development of a chemocline between anoxic ferruginous deep waters and anoxic sulphidic shallower waters during the mantle-plume breakout events that caused hydrothermal venting and subaerial volcanism. Hydrothermal venting provided abundant iron to deep waters resulting in iron-formation deposition and volcanism-provided sulphur (pyrite) and nitrogen to shallower environments causing an increase in productivity and the deposition of carbonaceous rich shale (Bekker et al., 2010).

Accordingly, it would appear that the rock types present at Totnes Road Fiord record a deepening event after volcanism as the iron-formation is deposited on top of the pyrite-bearing shale. In other locations, such as Mermaid Fiord and Moonshine Fiord, the iron-formation is overlain by another package of semipelitic rocks indicating a return to clastic sedimentation.

## CONCLUSIONS

A fragmental komatiitic suite exposed at Totnes Road Fiord, Cumberland Peninsula, eastern Baffin Island has been subdivided into eight separate units based on textural differences. The fragmental character of these komatiitic rocks which are Al-undepleted, Ti-enriched, and HFSE-enriched is consistent with being classified as Karasjok-type. Their Al-undepleted nature is attributed to melting of mantle at depths <250 km, depths too shallow for majorite garnet to be stable in the residue. Enrichment in Ti and other HFSEs can be explained by retention of a portion of the initial melt or by assimilation of metasomatized mantle or basaltic melts upon ascent. The fragmental character of this suite attests to its ultimate explosive eruption into relatively shallow water, <200 m deep, allowing fragmentation potentially through a combination of increased volatile content and steam explosivity. The presence of this distinctive volcanic package signals the possibility that a rising mantle plume impacted this region in Paleoproterozoic time, and may have had a role in rifting of Archean continental crust. The basin, which collected clastic detritus prior to volcanism, was the locus for later chemical and clastic sedimentation.

Ongoing geochemical and geochronological work will explore whether the Totnes Road Fiord section can be correlated with other volcanic-bearing supracrustal sequences of northeastern Cumberland Peninsula. These sequences will be compared with other Paleoproterozoic basin deposits, such as the Piling and Lake Harbour groups, in the Baffin Island region of the Canadian Shield to better constrain the architecture and tectonic evolution of this part of the shield.

## ACKNOWLEDGMENTS

The authors would like to thank Joe Whalen, Dave Lentz, John Percival, Marc St-Onge, Don James, and Brett Hamilton for discussions in the field. Additional assistance in the field was provided by Carl Nagy, Greg Dobbelsteyn, Norm Kopalie, and the rest of the Cumberland Peninsula Integrated Geoscience (GPIG) crew. Funding for this project was provided through Natural Resources of Canada's Geomapping for Energy and Minerals (GEM) program, a Natural Sciences and Engineering Research Council of Canada (NSERC) Discovery Grant to K. Ansdell, and a University of Saskatchewan Graduate Scholarship to R. Keim. Blaine Novakovski and Tim Prokopiuk in the Department of Geological Sciences at the University of Saskatchewan are thanked for thin-section preparation, and for geological discussions, respectively. This paper was reviewed and improved by John Percival.

## REFERENCES


Arndt, N.A., 2008. Komatiite; Cambridge University Press, Cambridge, United Kingdom, 488 p.

Arndt, N.T. and Nisbet, E.G., 1982. What is a komatiite?; *in* Komatiites, (ed.) N.T. Arndt and E.G. Nisbet; George Allen and Unwin, London, United Kingdom, p. 19–27.

Barley, M.E., Kerrich, R., Reudavy, I., and Xie, Q., 2000. Late Archaean Ti-rich, Al-depleted komatites and komatiitic volcaniclastic rocks from the Murchison Terrane in Western Australia; Australian Journal of Earth Sciences, v. 47, p. 873–883. doi:10.1046/j.1440-0952.2000.00820.x

Barnes, S. and Often, M., 1990. Ti-rich komatiites from northern Norway; Contributions to Mineralogy and Petrology, v. 105, p. 42–54. doi:10.1007/BF00320965

Bekker, A., Slack, J.F., Planavsky, N., Krapež, B., Hofmann, A., Konhauser, K.O., and Rouxel, O.J., 2010. Iron formation: The sedimentary product of a complex interplay among mantle, tectonic, oceanic, and biospheric processes; Economic Geology and the Bulletin of the Society of Economic Geologists, v.s 105, p. 467–508. doi:10.2113/gsecongeo.105.3.467

Beswick, A.E., 1982. Some geochemical aspects of alteration, and genetic relations in komatiitic suites; *in* Komatiites, (ed.) N.T. Arndt and E.G. Nisbet; George Allen and Unwin, London, United Kingdom, p. 283–308.

Capdevila, R., Arndt, N., Letendre, J., and Sauvage, J.-F., 1999. Diamonds in volcaniclastic komatiite from French Guiana; Nature, v. 399, p. 456–458. doi:10.1038/20911

Chavagnac, V., 2004. A geochemical and Nd isotopic study of the Barberton komatiites (South Africa): Implication for the Archean mantle; Lithos, v. 75, p. 253–281. doi:10.1016/j.lithos.2004.03.001

Corrigan, D., Scott, D.J., and St-Onge, M.R., 2001. Geology of the northern margin of the Trans-Hudson Orogen (Foxe Fold Belt), central Baffin Island, Nunavut; Geological Survey of Canada, Current Research 2001-C23, 27 p.

Corrigan, D., Pehrsson, S., Wodicka, N., and de Kemp, E., 2009. The Palaeoproterozoic Trans-Hudson Orogen: a prototype of modern accretionary processes; Geological Society of London; Special Publications, v. 327, p. 457–479. doi:10.1144/SP327.19

Coyle, M., 2009a. Residual total magnetic field, Cumberland Peninsula aeromagnetic survey, NTS 16 L South, Nunavut; Geological Survey of Canada, Open File 6092, scale 1:100 000.

Coyle, M., 2009b. Residual total magnetic field, Cumberland Peninsula aeromagnetic survey, parts of NTS 16 K North and 16 L North, Nunavut; Geological Survey of Canada, Open File 6094, scale 1:100 000.

Coyle, M., 2009c. First vertical derivative of the magnetic field, Cumberland Peninsula aeromagnetic survey, NTS 16 L South, Nunavut; Geological Survey of Canada, Open File 6101, scale 1:100 000.

Dyke, A.S., in press a. Surficial geology, Hoare Bay north, Baffin Island, Nunavut; Geological Survey of Canada, Canadian Geoscience Map 17, scale 1:100 000.

Dyke, A.S., in press b. Surficial geology, Pangnirtung south, Baffin Island, Nunavut; Geological Survey of Canada, Canadian Geoscience Map 19, scale 1:100 000.

Dyke, A.S., in press c. Surficial geology, Cape Dyer south, Baffin Island, Nunavut; Geological Survey of Canada, Canadian Geoscience Map 20, scale 1:100 000.

Elkins-Tanton, L.T., Draper, D.S., Agee, C.B., Jewell, J., Thorpe, A., and Hess, P.C., 2006. The last lavas erupted during the main phase of the Siberian flood volcanic province: results from experimental petrology; Contributions to Mineralogy and Petrology, v. 153, p. 191–209. doi:10.1007/s00410-006-0140-1

Fan, J. and Kerrich, R., 1997. Geochemical characteristics of aluminum depleted and undepleted komatiites and HREE-enriched low-Ti tholeiites, western Abitibi greenstone belt: A heterogeneous mantle plume-convergent margin environment; Geochimica et Cosmochimica Acta, v. 61, p. 4723–4744. doi:10.1016/S0016-7037(97)00269-X

Fowler, A.D., Berger, B., Shore, M., Jones, M.I., and Ropchan, J., 2002. Supercooled rocks: development and significance of varioles, spherulites, dendrites and spinifex in Archean volcanic rocks, Abitibi Greenstone Belt Canada; Precambrian Research, v. 115, p. 311–328. doi:10.1016/S0301-9268(02)00014-1

Fowler, A.D., Jensen, L.S., and Peloquin, S.A., 1987. Varioles in Archean basalts: products of spherultic crystallization; Canadian Mineralogist, v. 25, p. 275–289.

Gammon, P., Dyke, A., Sanborn-Barrie, M., and Young, M., 2011. Geochemistry and physical properties of till samples collected in 2009 from Cumberland Peninsula, Nunavut; Geological Survey of Canada, Open File 6763, 1 CD ROM.

Gangopadhyay, A., Walker, R.J., Hanski, E., and Solheid, P.A., 2005. Origin of Paleoproterozoic komatiites at Jeesiörova, Kittilä Greenstone complex, Finnish Lapland; Journal of Petrology, v. 47, p. 773–789. doi:10.1093/petrology/egi093

Gélinas, L., Trzcienski, W.E., and Brooks, C., 1976. Archean variolites – quenched immiscible liquids; Canadian Journal of Earth Sciences, v. 13, p. 210–230. doi:10.1139/e76-024

Hanski, H., Huhma, H., Rastas, P., and Kamenetsky, V.S., 2001. The Palaeoproterozoic komatiite-picrite association of Finnish Lapland; Journal of Petrology, v. 42, p. 855–876. doi:10.1093/petrology/42.5.855

Herzberg, C., 1995. Generation of plume magmas through time: an experimental perspective; Chemical Geology, v. 126, p. 1–16. doi:10.1016/0009-2541(95)00099-4

Jackson, G.D. and Taylor, F.C., 1972. Correlation of major Aphebian rock units in the Northeastern Canadian Shield; Canadian Journal of Earth Sciences, v. 9, p. 1650–1669. doi:10.1139/e72-146

Johns, S.M., Helmstaedt, H.H., and Kyser, T.K., 2006. Paleoproterozoic submarine intrabasinal rifting, Baffin Island, Nunavut, Canada: volcanic structure and geochemistry of the Bravo Lake Fromation; Canadian Journal of Earth Sciences, v. 43, p. 593–616. doi:10.1139/e06-009

Kalfoun, F., Ionov, D., and Merlet, C., 2002. HFSE residence and Nb/Ta ratios in metasomatised, rutile-bearing mantle peridotites; Earth and Planetary Science Letters, v. 199, p. 49–65. doi:10.1016/S0012-821X(02)00555-1

Kokelaar, P., 1986. Magma-water interactions in subaqueous and emergent basaltic volcanism; Bulletin of Volcanology, v. 48, p. 275–289. doi:10.1007/BF01081756

Nesbit, R.W., Sun, S.S., and Purvis, A.C., 1979. Komatiites: geochemistry and genesis; Canadian Mineralogist, v. 17, p. 165–186.

Pearce, J.A., 1996.A user's guide to basalt discrimination diagrams, *in* Trace element geochemistry of volcanic rocks: applications for massive sulphide exploration, (ed.) D.A. Wyman; Geological Association of Canada, Short Course Notes, v. 12, p. 79–113.

Pyke, D.R., Naldrett, A.J., and Eckstrand, O.R., 1973. Archean ultramafic flows in Munro Township, Ontario; Geological Society of America Bulletin, v. 84, p. 955–978. doi:10.1130/0016-7606(1973)84<955:AUFIMT>2.0.CO;2

Sanborn-Barrie, M., Young, M., Whalen, J., St-Onge, M.R., James, D., Rayner, N., Coyle, M., Lynds, T., and Hilary, B., 2010. A new bedrock geology map of the Cumberland Peninsula, Nunavut: an initial step in evaluating the mineral potential of eastern Baffin Island; 38th Annual Yellowknife Geoscience Forum Abstracts; Northwest Territories Geoscience Office, Yellowknife, NT. YKGSF Abstracts Volume 2010.

Sanborn-Barrie, M., St-Onge, M.R., Young, M.D., and James, D.T., 2008. Bedrock geology of southwestern Baffin Island, Nunavut: expanding the tectonostratigraphic framework with relevance to mineral resources; Geological Survey of Canada Current Research 2008–6, 16 p.

Sanborn-Barrie, M., Young, M., Whalen, J., and James, D., 2011. Geology, Ujuktuk Fiord Nunavut; Geological Survey of Canada, Canadian Geoscience Map 1 (preliminary version) scale 1:100 000.

Schaefer, S.J. and Morton, P., 1991. Two komatiitic pyroclastic units, Superior Province, northwestern Ontario: their geology, petrography, and correlation; Canadian Journal of Earth Sciences, v. 28, p. 1455–1470. doi:10.1139/e91-128

Scott, D.J., St-Onge, M.R., and Corrigan, D., 2002. Geology of the Paleoproterozoic Piling Group and underlying Archean gneiss, central Baffin Island, Nunavut; Geological Survey of Canada, Current Research 2002-C17, 10 p.

Sohn, R.A., Willis, C., Humphris, S., Shank, T.M., Singh, H., Edmonds, H.N., Kunz, C., Hedman, U., Helmke, E., Jakuba, M., Liljebladh, B., Linder, J., Murphy, C., Nakamura, K.-I., Sato, T., Schlindwein, V., Stranne, C., Tausenfreund, M., Upchurch, L., Winsor, P., Jakobsson, M., and Soule, A., 2008. Explosive volcanism on the ultraslow-spreading Gakkel ridge, Arctic Ocean; Nature, v. 453, p. 1236–1238. doi:10.1038/nature07075

Smye, A.J., St-Onge, M.R., and Waters, D.J., 2009. Contrasting metamorphic pressure-temperature histories within the Trans-Hudson Orogen's hinterland, southwest Baffin Island, Nunavut; Geological Survey of Canada, Current Research 2009-6, 18 p.

St-Onge, M.R., Jackson, G.D., and Henderson, I., 2006a. Geology, Baffin Island (south 70°N and east of 80°W), Nunavut; Geological Survey of Canada, Open File 4931, scale 1:500 000. .

St-Onge, M.R., Searle, M.P., and Wodick, N., 2006b. Trans-Hudson Orogen of North America and Himalaya-Karakoram-Tibetan Orogen of Asia: structural and thermal characteristics of the lower and upper plates; Tectonics, v. 25, 22 p. doi:10.1029/2005TC001907

St-Onge, M.R., Van Gool, J., Garde, A.A., and Scott, D.J., 2009. Correlation of Archaean and Palaeoproterozoic units between northeastern Canada and western Greenland: constraining the pre-collisional upper plate accretionary history of the Trans-Hudson orogen; Geological Society of London; Special Publications, v. 318, p. 193–235. doi:10.1144/SP318.7

Sun, S.S. and McDonough, W.F., 1989. Chemical and isotopic systematics of oceanic basalts: implications for mantle composition and processes; *in* Magmatism in the ocean basins, (ed.) A.D. Saunders and M.J. Norry; Geological Society of London, Special Publications, v. 42, p. 313–345.

Tomlinson, K.Y., Hughes, D.J., Thurston, P.C., and Hall, R.P., 1999. Plume magmatism and crustal growth at 2.9 to 3.0 Ga in the Steep Rock and Lumby Lake area, Western Superior Province; Lithos, v. 46, p. 103–136. doi:10.1016/S0024-4937(98)00057-7

Viljoen, M.J. and Viljoen, R.P., 1969. The geology and geochemistry of the lower ultramafic unit of the Onverwacht Group and a proposed new class of igneous rocks; Geological Society of South Africa; Special Publication, v. 21, p. 55–85.

Viljoen, M.J., Viljoen, R.P., Smith, H.S., and Erlank, A.J., 1983. Geological, textural and geochemical features of komatiitic flows from the Komati Formation; Geological Society of South Africa; Special Publication, v. 9, p. 1–20.

Wagner, T.P. and Grove, T.L., 1997. Experimental constraints on the origin of lunar high-Ti ultramafic glasses; Geochimica et Cosmochimica Acta, v. 61, p. 1315–1327. doi:10.1016/S0016-7037(96)00387-0

Xie, Q., Kerrich, R., and Fan, J., 1993. HFSE/REE fractionations recorded in three komatiite-basalt sequences, Archean Abitibi Greenstone Belt; implications for multiple plume sources and depths; Geochimica et Cosmochimica Acta, v. 57, p. 4111–4118. doi:10.1016/0016-7037(93)90357-3

Geological Survey of Canada Project MGM007